Supplement of Earth Syst. Sci. Data, 16, 3453–3470, 2024
https://doi.org/10.5194/essd-16-3453-2024-supplement

Open Access Earth System Science Data

Supplement of

Annual time-series 1 km maps of crop area and types in the conterminous US (CropAT-US): cropping diversity changes during 1850–2021

Shuchao Ye et al.

Correspondence to: Chaoqun Lu (clu@iastate.edu)

Table S1. The reclassification of CDL. [1] and [2] are the crop type ID used in CDL and this study, respectively.

CDL[1]	This study[2]	Crop type
1	1	Corn
5	2	Soybean
24	3	Winter wheat
23	4	Spring wheat
22	5	Durum wheat
2	6	Cotton
4	7	Sorghum
21	8	Barley
3	9	Rice
Other crop types	10	Others

Table S2. The earliest available dates of harvesting and planting area for nine major crops at state and county level from USDA-NASS Quick Stats.

Crop Type	State Harvest	State Plant	County Harvest	County Plant
Corn	1866	1919	1910	1924
Soybean	1924	1924	1927	1938
Winter Wheat	1909	1909	1918	1919
Spring Wheat	1919	1919	1919	1919
Durum Wheat	1919	1924	1926	1926
Cotton	1866	1909	1919	1928
Sorghum	1919	1924	1940	1940
Rice	1895	1929	1938	1953
Barley	1866	1924	1915	1924

Table S3. The mean corn-soybean ration ratio calculated from the available years.

State	Rotation Rate (%)	Standard Deviation	State	Rotation Rate (%)	Standard Deviation
IL	85	5	MO	58	8
IN	81	10	NB	59	12
IA	86	5	NC	30	10
KS	35	9	OH	64	12
KY	58	15	PA	27	10
LA	16	10	SD	69	7
MI	49	11	TN	35	15
MN	74	6	WI	43	13
MS	14	9			

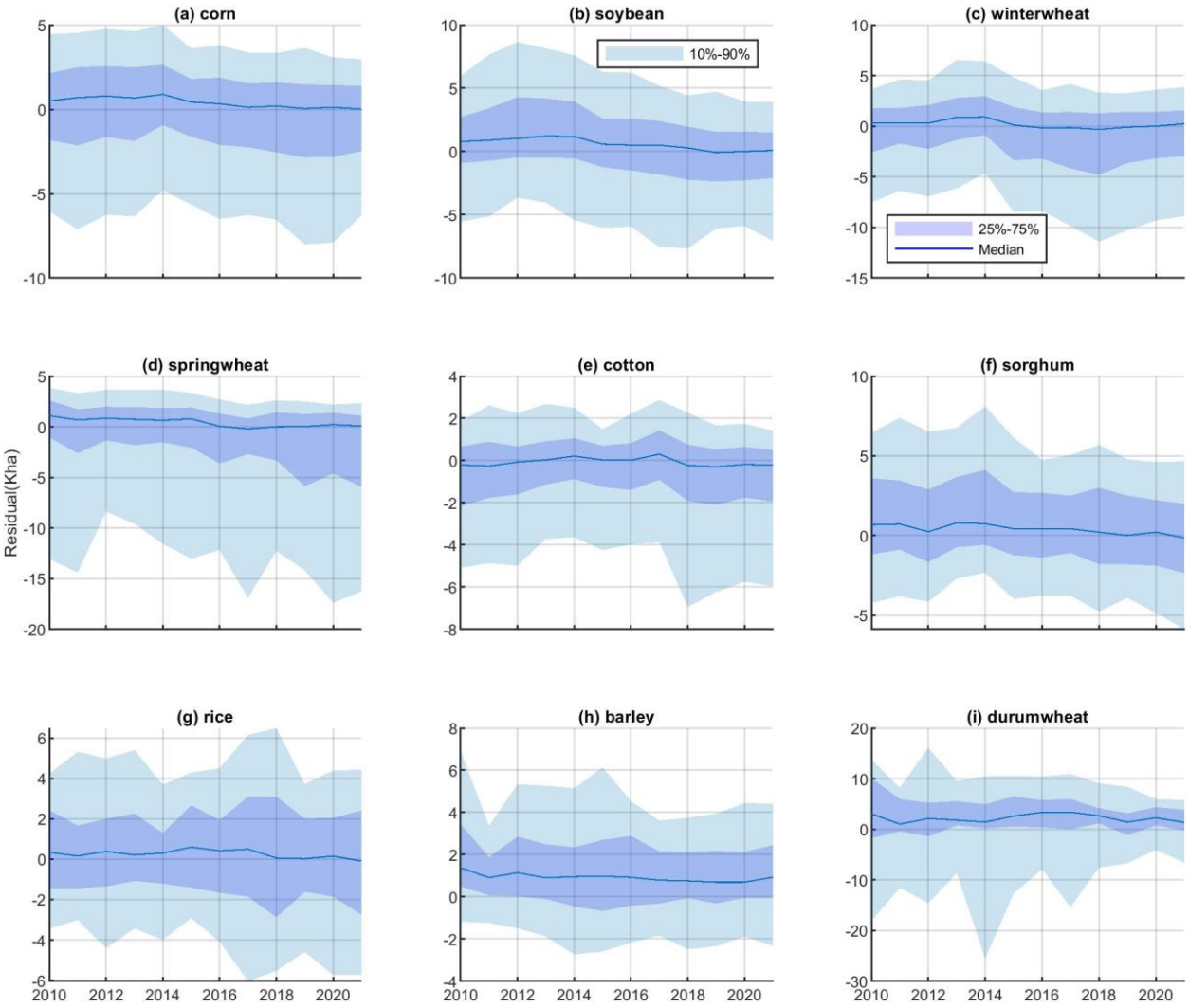

Figure S1. The distribution of residual (the inventory-based crop area minus the CDL-based crop area, defined by Equation 6) between the USDA Quick Stats and CDL from 2010 to 2021 (Kha is a thousand hectares). In each year, "10%-90%", "Median", and "25%-75%", reflect the extent of residual at levels of "10th percentile to 90th percentile", "50th percentile", and "25th percentile to 75th percentile", respectively.

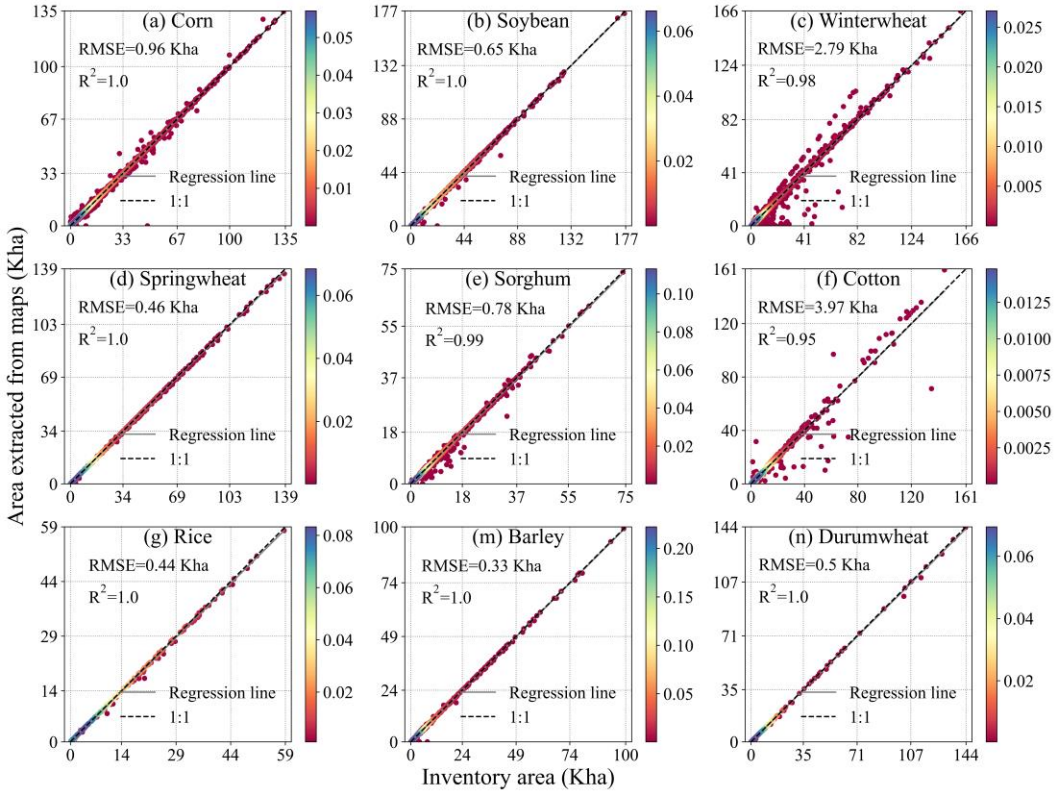

Figure S2. Comparison of crop-specific cropland area between reconstructed maps and raw inventory data at county level in 1920, 1960, 2000, and 2020 (Kha is a thousand hectares). The point in subfigures represents the paired cropland area from the reconstructed map and raw inventory data for a certain county and year. The color bar in each subfigure indicates the probability density of paired point calculated by the gaussian kernel.

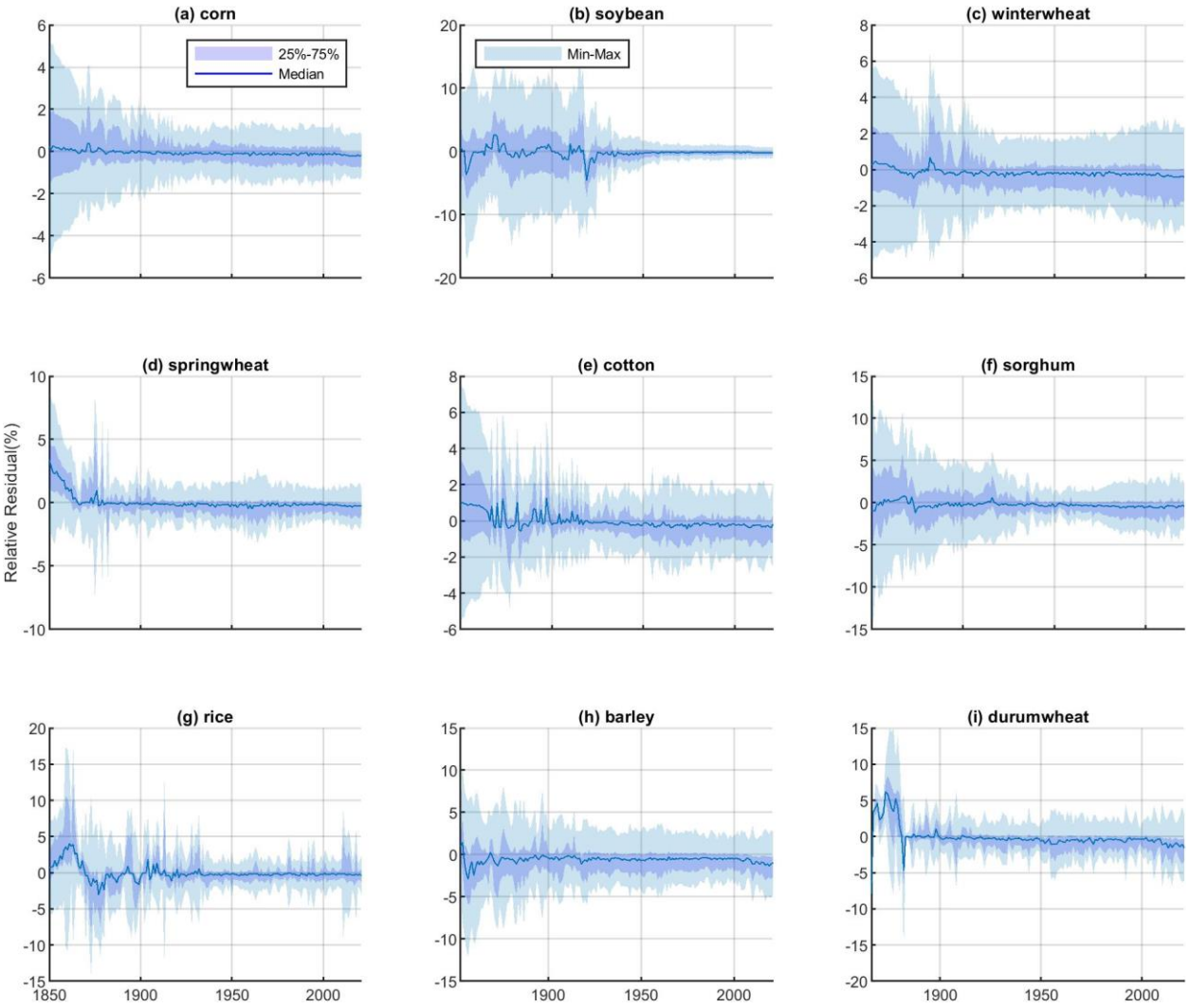

Figure S3. The distribution of relative residual (the ratio of the residual to the inventory crop area, defined by Eq. 7) between the rebuilt inventory and rebuilt maps from 1850 to 2021. In each year, “Min–Max”, “Median”, and “25%–75%” reflect the extent of residual at levels of “minimum value to maximum value”, “50th percentile”, and “25th percentile to 75th percentile”, respectively. The counties with the total cropland areas less than 1kha are excluded to avoid the case with a relative residual greater than 100%.

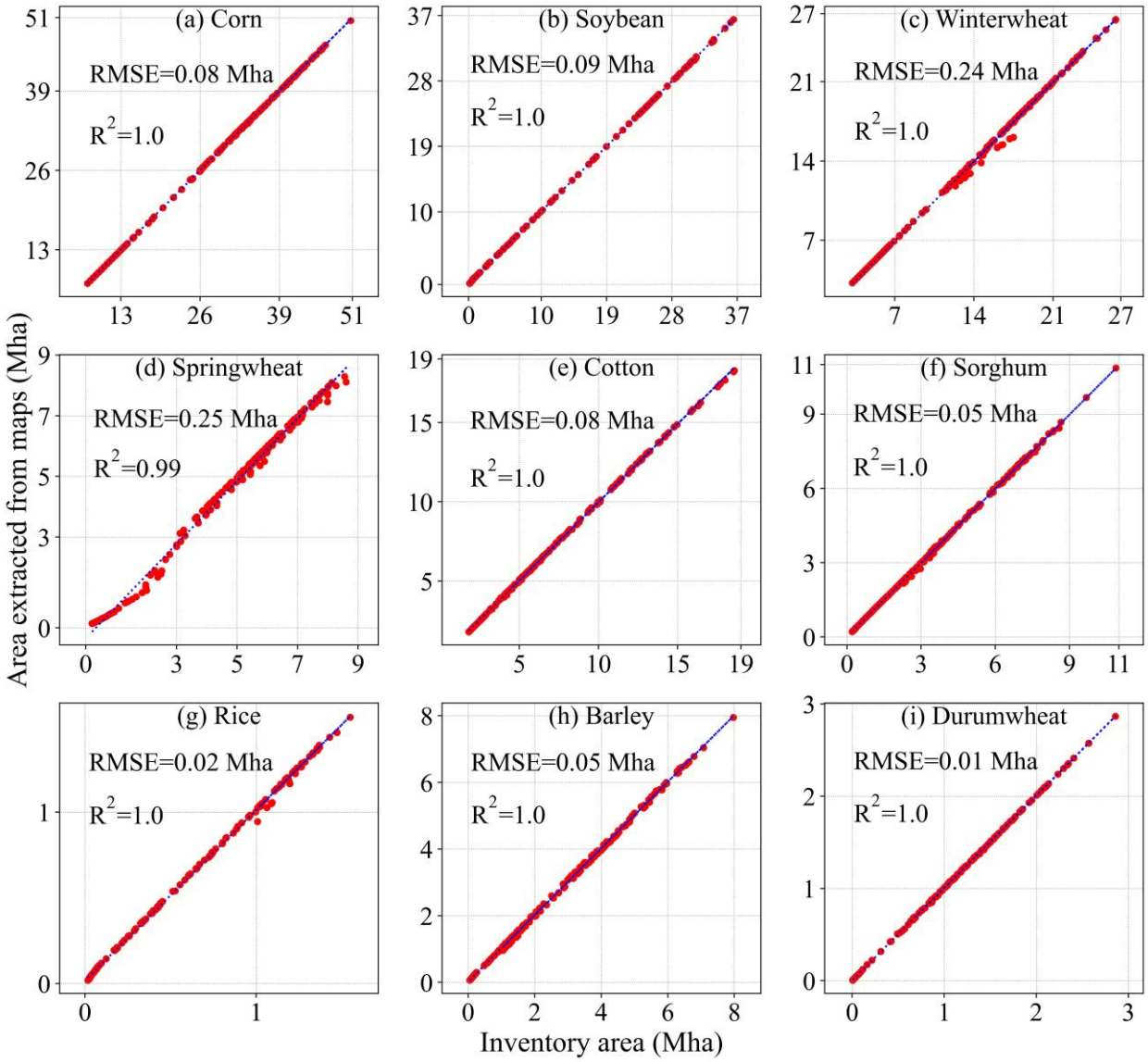

Figure S4. The crop type-specific comparison of total US crop area between the developed map and the rebuilt inventory data from 1850 to 2021 (Mha is a million hectares). The blue line is the linear regression line.

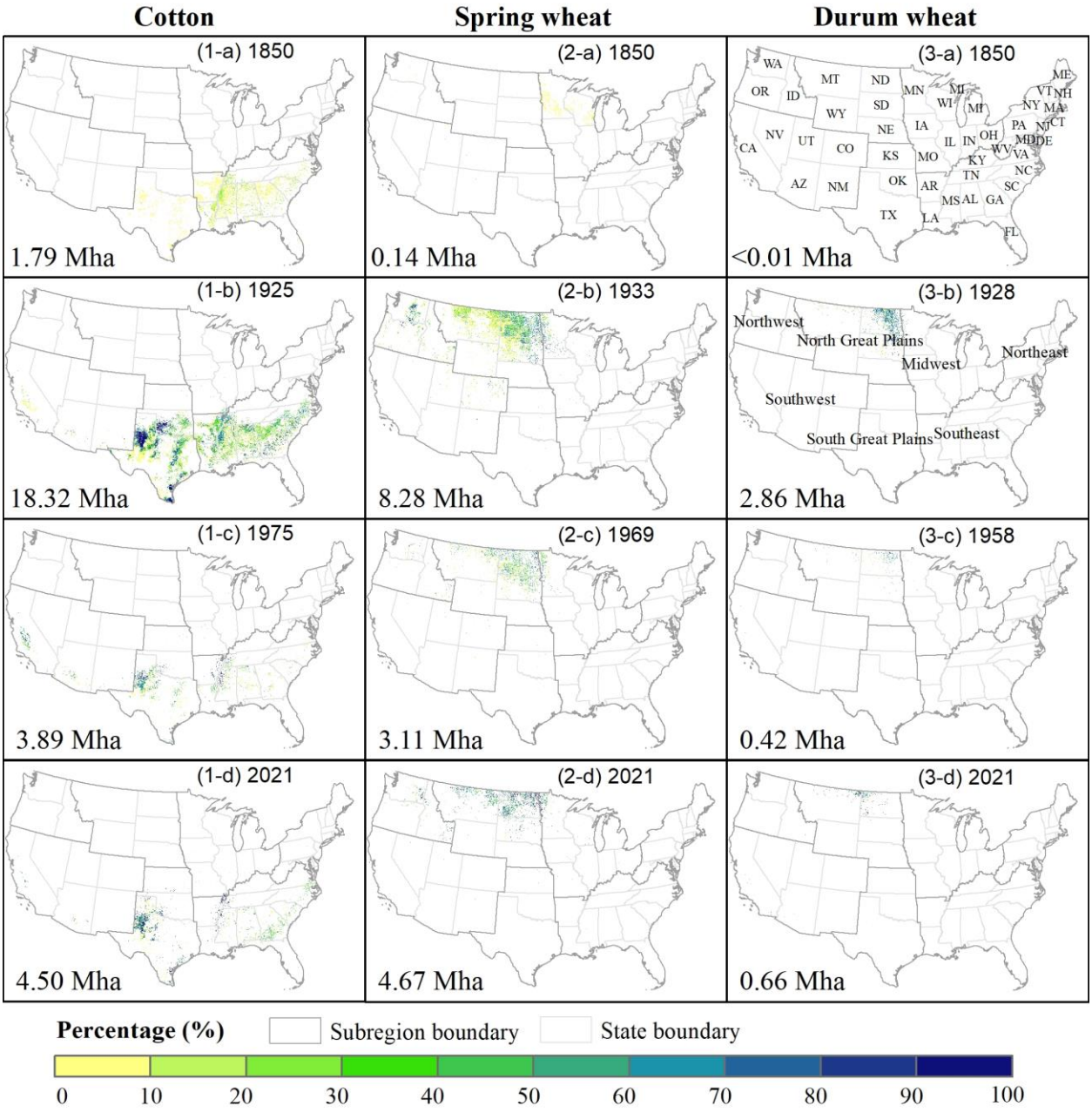

Figure S5. The spatiotemporal density pattern of cotton, spring wheat, and durum wheat at a 1km × 1km resolution in the turning point years with abrupt area changes. The first, second, and third columns are the density patterns of cotton, spring wheat, and durum wheat, respectively. The total planting area for each crop type is presented at the bottom left of each panel. The color bar at the bottom indicates the percentage of planting area to the total grid area.

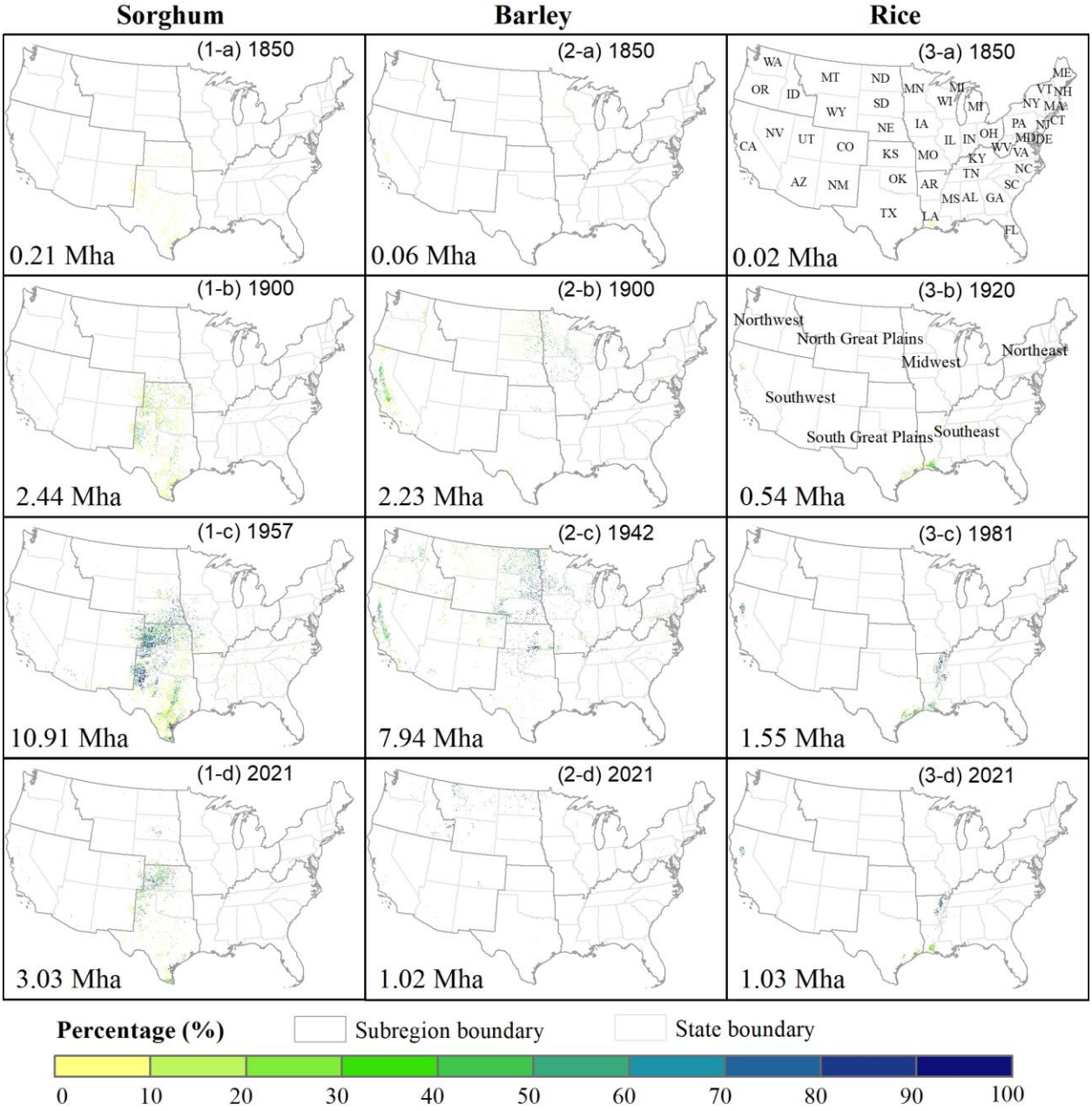

Figure S6. The spatiotemporal density pattern of sorghum, barley, and rice at a 1km × 1km resolution in the turning point years with abrupt area changes. The first, second, and third columns are the density patterns of sorghum, barley, and rice, respectively. The total planting area for each crop type is presented at the bottom left of each panel. The color bar at the bottom indicates the percentage of planting area to the total grid area.

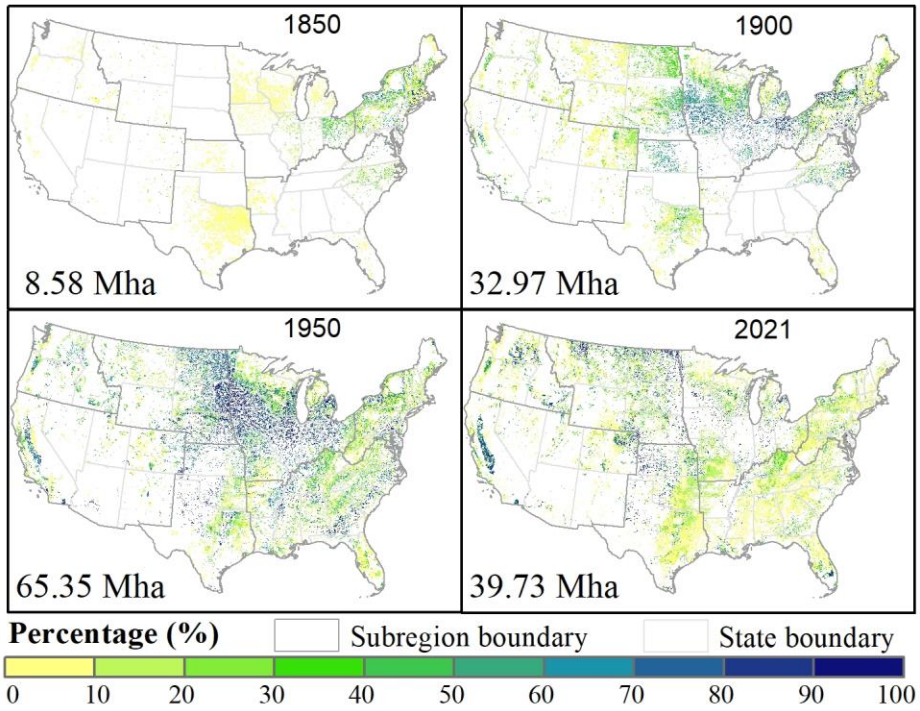

Figure S7. The spatiotemporal density patterns of "others". The color bar at the bottom indicates the percentage of planting area to the total grid area.

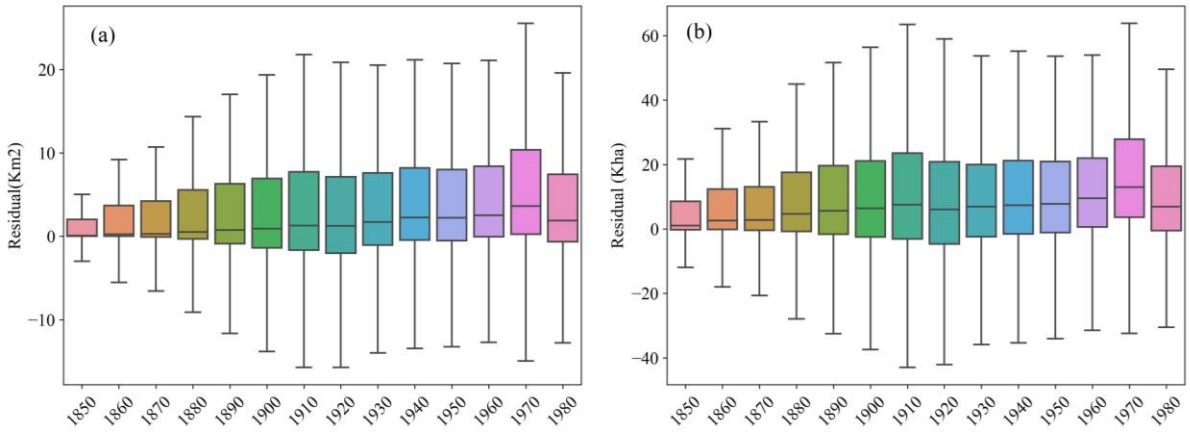

Figure S8. The distribution of residual between HYDE and our maps at pixel (a) and county (b) level.

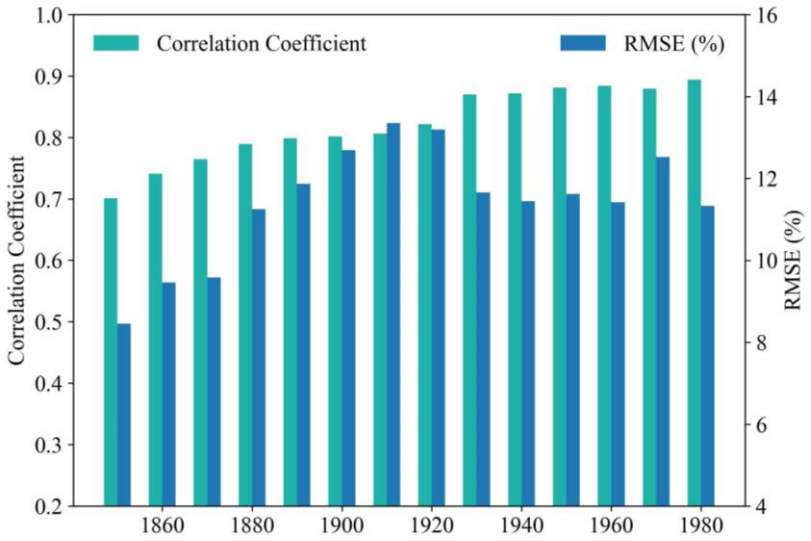

Figure S9. Comparison of cropland proportion in the corresponding pixels between HYDE and our products. Our maps are aggregated to the same resolution as HYDE.

Supplementary Methods:

(1) Preprocesses for LCMAP

Figure S10 shows that the total US cropland from LCMAP is significantly greater than that from NLCD and the inventory data due to its more extensive spatial coverage (Figure S11 (a) and (b)). By checking the product guide of LCMAP, NLCD uses a finer-grained Anderson Level II-based legend, in contrast to LCMAP's broader Level I-derived classes, where the classification of NLCD can be cross-walked to LCMAP classes (Table S4) (United States Geological Survey, 2022; Xian et al., 2022). Thus, the cropland in LCMAP refers to the pasture and cropland in NLCD, which is also confirmed by the result in Figure S10 where the sum of crop and pasture from NLCD is close to LCMAP's cropland area. Based on that, we adopted the NLCD-based trajectory method to filter the real cropland pixels from LCMAP. We first reclassified NLCD land cover maps into two classes, crop and non-crop from 2001 to 2011. Then, we used Equations S1 to stack the reclassed maps into a single in which each value, representing a trajectory, records the historical crop states (Figure S12). To retain the potential cropland distribution in LCMAP, we apply the selected non-crop trajectory (Figure S12) to exclude all grids identified as cropland in LCMAP from 1985 to 2009, where we assume that the non-crop grids in NLCD from 2001 to 2011 keep non-crop between 1985 and 2000. The filtered LCMAP is presented in Figure S11 (c) (Taking the year 2008 as a case).

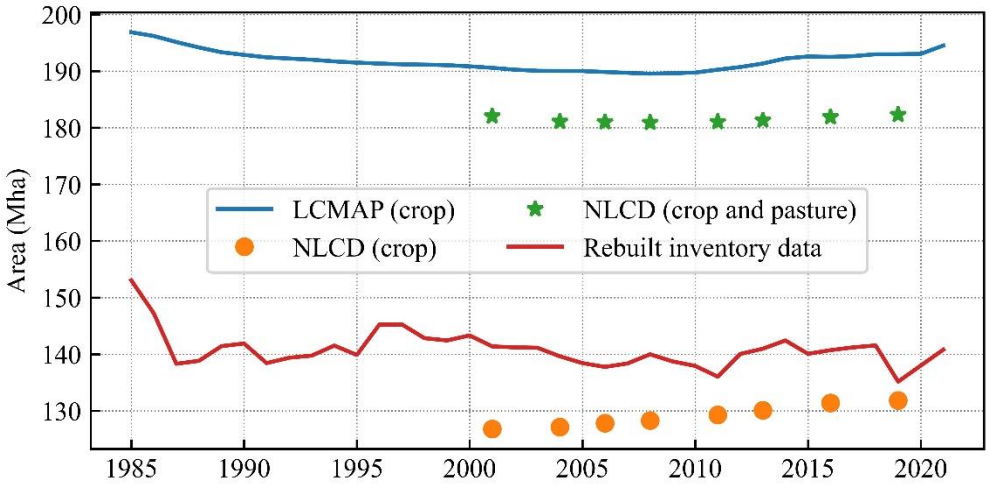

Figure S10. The total US cropland area trends extracted from the resampled LCMAP, NLCD, and the rebuilt inventory data, respectively.

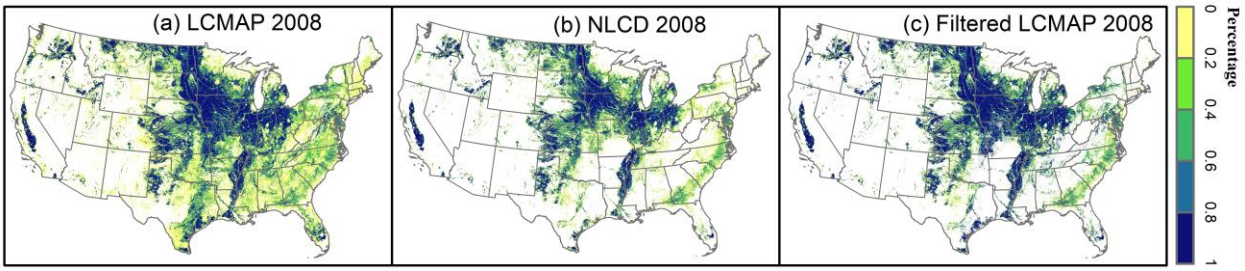

Figure S11. The distribution of the resampled LCMAP (a), NLCD (b), and filtered LCMAP (c). Taking the year 2008 as a case to show the spatial pattern.

Table S4. NLCD to LCMAP land cover translations (United States Geological Survey, 2022; Xian et al., 2022).

NLCD Level 2 Class	LCMAP Level 1 Class
Developed, Open Space Developed, Low Intensity Developed, Medium Intensity Developed, High Intensity	Developed
Pasture/Hay Cultivated crops	Cropland
Dwarf Scrub Shrub/Scrub Grassland/Herbaceous Sedge/Herbaceous Lichens Moss	Grass/Shrub
Deciduous Forest Evergreen Forest Mixed Forest	Tree Cover
Open Water	Water
Woody wetlands Emergent Herbaceous Wetlands	Wetlands
Perennial Ice/Snow	Ice/Snow
Barren Land	Barren

$$Croptrac = \sum_1^5 (NLCD_i * 10^{5-i}), \quad \text{(S1)}$$

Where,

$Croptrac$: the crop trajectory, the meaning of which is shown in Figure S12;

Cl_i: the reclassed NLCD map in the year from 2001 (i =1) to 2011 (i =5).

	2001	2004	2006	2008	2011
Crop	*	*	1	*	*
Non-crop	0	0	0	0	0

Figure S12. Example of crop trajectory. 1 and 0 represent crop and non-crop, respectively. * is either 1 or 0. Non-crop trajectory means that this pixel keeps non-crop from 2001 to 2011.

(2) Linear interpolation in HYDE

Here, the linear algorithm (Equation S2) is used to interpolate the potential cropland map in years when HYDE was unavailable before 1985.

$$A_{x,y}^{t_i} = \frac{A_{x,y}^{t_2} - A_{x,y}^{t_1}}{t_2 - t_1} \times (t_i - t_1) + A_{x,y}^{t_1} \quad \text{(S2)}$$

Where,

t_2 and t_1 are two adjacent years when HYDE is available, assuming t_2 is greater than t_1;

t_i is any year between t_1 and t_2;

$A_{x,y}^{t_2}$, $A_{x,y}^{t_1}$ are the HDYE cropland percentage for the location (x, y) in year t_2 and t_1, respectively.

$A_{x,y}^{t_i}$ is the interpolated cropland percentage in the year t_i at (x, y).

Reference:

United States Geological Survey: Land change monitoring, assessment, and projection (LCMAP 1.3) Science Product Guide, U.S. Geological Survey Fact Sheet, https://doi.org/10.3133/ fs20203024, 2022.

Xian, G. Z., Smith, K., Wellington, D., Horton, J., Zhou, Q., Li, C., Auch, R., Brown, J. F., Zhu, Z., and Reker, R. R.: Implementation of the CCDC algorithm to produce the LCMAP Collection 1.0 annual land surface change product, Earth Syst. Sci. Data, 14, 143–162, https://doi.org/10.5194/essd-14-143-2022, 2022.